

DopQ-ViT: Towards Distribution-Friendly and Outlier-Aware Post-Training Quantization for Vision Transformers

Lianwei Yang^{1,2}, Haisong Gong^{1,2}, Qingyi Gu^{1,*}

¹Institute of Automation, Chinese Academy of Sciences

²School of Artificial Intelligence, University of Chinese Academy of Sciences

Abstract

Vision transformers (ViTs) have garnered significant attention for their performance in vision tasks, but the high computational cost and significant latency issues have hindered widespread adoption. Post-training quantization (PTQ), a promising method for model compression, still faces accuracy degradation challenges with ViTs. There are two reasons for this: the existing quantization paradigm does not fit the power-law distribution of post-Softmax activations well, and accuracy inevitably decreases after reparameterizing post-LayerNorm activations. We propose a **Distribution-Friendly and Outlier-Aware Post-training Quantization** method for Vision Transformers, named **DopQ-ViT**. DopQ-ViT analyzes the inefficiencies of current quantizers and introduces a distribution-friendly Tan Quantizer called TanQ. TanQ focuses more on values near 1, more accurately preserving the power-law distribution of post-Softmax activations, and achieves favorable results. Besides, during the reparameterization of post-LayerNorm activations from channel-wise to layer-wise quantization, the accuracy degradation is mainly due to the significant impact of outliers in the scaling factors. Therefore, DopQ-ViT proposes a method to select Median as the Optimal Scaling Factor, denoted as MOSF, which compensates for the influence of outliers and preserves the performance of the quantization model. DopQ-ViT has been extensively validated and significantly improves the performance of quantization models, especially in low-bit settings.

Introduction

Vision Transformers have demonstrated strong capabilities in image classification (Bhojanapalli et al. 2021; Chen, Fan, and Panda 2021), object detection (Li et al. 2022a; Carion et al. 2020), and instance segmentation (Wang et al. 2021; Chen et al. 2021), owing to the superiority of their self-attention mechanism. However, the performance of ViTs relies on extensive computations, leading to increased memory footprint, slower inference speed, and significant challenges in deploying them on edge devices. To address this challenge, several studies (Yu et al. 2022; Wu et al. 2022; Liu et al. 2021b) implement model compression through pruning, distillation, or quantization, aiming to accelerate inference speed and facilitate deployment on edge devices. Although these efforts have not achieved ideal results, they

have still laid a solid foundation for future work. As a practical and effective method of model compression, quantization (Gholami et al. 2022; Krishnamoorthi 2018) significantly reduces the model’s complexity by representing weights and activations in lower bits. Previous quantization has focused on Quantization-Aware Training (QAT) (Nagel et al. 2022; Esser et al. 2019; Choi et al. 2018; Gong et al. 2019; Li and Gu 2023; Liu, Liu, and Cheng 2023; Li et al. 2022b,d; Zhong et al. 2022, 2023b), which involves end-to-end retraining using the entire training set. Although QAT compensates for the accuracy degradation caused by quantization, the computational resources and time required hinder its further development. Post-Training Quantization (PTQ) (Li et al. 2022c; Ding et al. 2022; Frumkin, Gope, and Marculescu 2023; Li et al. 2023a; Lin et al. 2022; Zhong et al. 2023a; Li et al. 2023b; Banner, Nahshan, and Soudry 2019; Yuan et al. 2022; Liu et al. 2021b) requires only a small dataset to calibrate the pre-trained model, avoiding complex retraining and providing convenience for deployment.

However, when quantizing ViTs to low-bit widths, the model may experience accuracy degradation or even fail completely. Our analysis suggests that there are two reasons behind the poor performance of low-bit quantization models. The limited quantization bit-width leads to increased quantization errors, thereby restricting the expressive power of the model. Moreover, existing quantization paradigms face challenges in handling the unique structures of ViTs, such as LayerNorm and Softmax. Therefore, some PTQ methods compensate for accuracy degradation through reconstruction techniques. Unlike QAT, reconstruction only requires a small amount of data and an acceptable time cost. After theoretical analysis and validation, BrecQ (Li et al. 2021) optimizes the model by minimizing block output errors. Qdrop (Wei et al. 2022a) introduces random dropout operations during block-wise reconstruction to update the parameters. Furthermore, some PTQ research studies have proposed specialized quantizers to handle specific structures in ViTs. To quantize post-Softmax activations, PTQ4ViT (Yuan et al. 2022) and FQ-ViT (Lin et al. 2022) propose the twin uniform quantizer and Log2 quantizer, respectively. APQ-ViT (Ding et al. 2022) introduces the Matthew-effect Preserving Quantization method (MPQ) to align with the data distribution. I&S-ViT (Zhong et al. 2023a) adopts the shift-uniform-log2 quantizer (SULQ) to enhance quantiza-

*Corresponding Author

tion efficiency. For post-LayerNorm activations, RepQ-ViT (Li et al. 2023b) applies channel-wise quantization to handle inter-channel variation, and reparameterizes it to layer-wise quantization to improve inference efficiency.

In this paper, we propose an efficient and accurate PTQ method for ViTs, named DopQ-ViT. DopQ-ViT takes into account the impact of specific structures in ViTs and optimizes the model through reconstruction. Log Quantizer focuses on precisely quantizing the values close to 0 in post-Softmax activations, while neglecting those close to 1, thereby limiting its performance. Therefore, our method DopQ-ViT proposes a distribution-friendly Tan Quantizer (TanQ) to improve quantization efficiency. For values near 1 in post-Softmax activations, TanQ can focus more on them and accurately fit the distribution. Besides, we observe a decrease in accuracy when transitioning post-LayerNorm activations from channel-wise quantization to layer-wise quantization. This is because a single scaling factor cannot accommodate all channels, especially those with significant range variations. DopQ-ViT proposes a method to select Median as the Optimal Scaling Factor, denoted as MOSF. MOSF uses the mean absolute deviation as an evaluation metric to determine the median as the optimal scaling factor, without introducing additional calculations. This scaling factor facilitates accurate quantization for most channels and compensates for errors caused by abnormal channels. Similar to I&S-ViT (Zhong et al. 2023a), DopQ-ViT also observes that activations are sensitive, which poses challenges for quantization. Therefore, our method DopQ-ViT first quantizes all activations and then completes the initial activation reconstruction, laying a solid foundation for subsequent work. Then, with the help of MOSF, we reparameterize the post-LayerNorm activations to achieve layer-wise quantization. Finally, we quantize all weights and perform reconstruction again to obtain the superior quantized model.

Our main contributions are summarized as follows:

- We have identified two issues with current post-training quantization methods for ViTs: First, existing quantizers do not align well with the distribution of post-Softmax activations. Second, accuracy decreases after reparameterizing the post-LayerNorm activations.
- We propose a novel PTQ method for ViTs, named DopQ-ViT. DopQ-ViT introduces the Tan Quantizer, which focuses more on values near 1, thereby better fitting the distribution of post-Softmax activations. Besides, DopQ-ViT employs MOSF to select the median as the optimal scaling factor, effectively addressing the accuracy degradation issue that occurs after reparameterizing post-LayerNorm activations.
- We evaluate DopQ-ViT on image classification and object detection tasks across various model variants and bit-settings. Compared to existing PTQ methods, DopQ-ViT demonstrates favorable performance.

Related Work

Vision Transformers

Vision Transformers (ViTs), based on the self-attention mechanism, have achieved significant success in visual tasks

such as image classification (Bhojanapalli et al. 2021; Chen, Fan, and Panda 2021), object detection (Li et al. 2022a; Carion et al. 2020), and instance segmentation (Wang et al. 2021; Chen et al. 2021). Compared to Convolutional Neural Networks (CNNs), ViTs can capture global information from the entire image more effectively and serve as superior vision backbones for tasks. ViT (Dosovitskiy et al. 2020) divides images into patches, treats them as sequential data, and employs the self-attention mechanism to analyze dependencies within the images. DeiT (Touvron et al. 2021) combines knowledge distillation with ViTs to reduce data dependency and achieve competitive results. Swin Transformer (Liu et al. 2021a) constructs a hierarchical vision transformer using shifted windows to efficiently handle features at different scales. Additionally, there are some extended works (Yuan et al. 2021; Liu et al. 2022) based on ViTs that have also demonstrated excellent performance.

Model Quantization

Model quantization can save memory and accelerate inference speed by representing floating-point parameters as integers. Post-Training Quantization (PTQ) does not require retraining the network to achieve more desirable model quantization. Therefore, PTQ has gained widespread attention in model compression, but maintaining accuracy advantages at low bit-widths remains challenging. Fortunately, the optimization-based PTQ methods can mitigate the accuracy degradation. BRECCQ (Li et al. 2021) proposes a block-wise reconstruction method to optimize model parameters. Qdrop (Wei et al. 2022a) enhances the usability of low-bit quantization by introducing activation quantization and dropout during reconstruction. Based on block-wise reconstruction, PD-Quant (Liu et al. 2023) also optimizes quantization parameters guided by global information from the full-precision model. MGRQ (Yang et al. 2024) proposes mixed granularity reconstruction quantization to enhance the accuracy of low-bit model quantization.

The special components in ViTs, such as Softmax and LayerNorm, constrain the quantization performance of the model. The uniform quantizer may not be suitable. Therefore, some studies have proposed more specific quantization paradigms. PTQ4ViT (Yuan et al. 2022) observes that the distribution of post-Softmax activations is different from the gaussian distribution, thus proposing the twin uniform quantization method to reduce errors. On this basis, FGPTQ-ViT (Liu, Shi, and He 2023) develops an adaptive piecewise point search algorithm to fit the distribution of post-Softmax activations more accurately. FQ-ViT (Lin et al. 2022) innovatively proposes the Log2 quantizer, which allocates more quantization intervals to denser regions of post-Softmax activations. RepQ-ViT (Li et al. 2023b) further introduces $\text{Log}\sqrt{2}$ quantization for post-Softmax activations with power-law features and subsequently reparameterizes it to Log2 quantization for inference. APQ-ViT (Ding et al. 2022) proposes the MPQ method, which preserves the Matthew effect of the Softmax output during the quantization process. I&S-ViT (Zhong et al. 2023a) proposes the shift-uniform-log2 quantizer (SULQ) to alleviate the quantization inefficiency inherent in the Log2 quantizer.

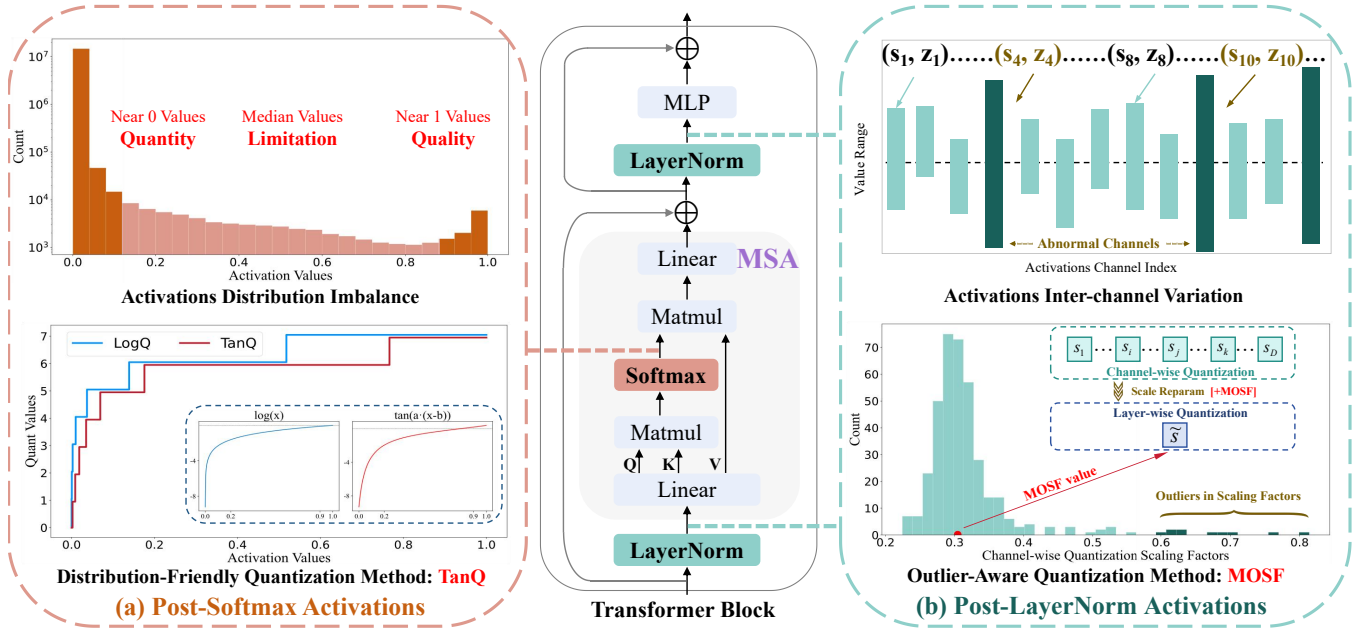


Figure 1: Overview of the proposed DopQ-ViT framework. DopQ-ViT proposes the distribution-friendly Tan Quantizer to address the imbalance in the distribution of post-Softmax activations, thereby enhancing the practicality of low-bit quantization. Additionally, DopQ-ViT proposes an outlier-aware method MOSF to address the inter-channel variation in post-LayerNorm activations, aiming to select the optimal scaling factor and mitigate accuracy degradation during the reparameterization process.

Methodology

Preliminaries

Structure of ViTs. Vision Transformers (ViTs) are formed by stacking multiple transformer encoder blocks. Each encoder is structured with a multi-head self-attention (MSA) module and a multi-layer perceptron (MLP) module. For an input image, ViTs initially divide it into N patches. Then, the embedding layer converts these patches into a sequence of D -dimensional vectors. This vector is fed into L transformer blocks to complete the subsequent operations. Specifically for the l_{th} block, when the input is X_l , the process is executed as follows:

$$Y_l = X_l + \text{MSA}(\text{LayerNorm}(X_l)) \quad (1)$$

$$X_{l+1} = Y_l + \text{MLP}(\text{LayerNorm}(Y_l)) \quad (2)$$

The MSA comprises h self-attention heads that capture correlations between patches. For the i_{th} head, when the input is X' , the process unfolds as follows:

$$[Q_i, K_i, V_i] = X' W^{QKV} + b^{QKV} \quad (3)$$

$$\text{Attn}_i = \text{Softmax} \left(\frac{Q_i \cdot K_i^T}{\sqrt{D_h}} \right) V_i \quad (4)$$

$$\text{MSA}(X') = [\text{Attn}_1, \text{Attn}_2, \dots, \text{Attn}_h] W^o + b^o \quad (5)$$

In MSA, the query (Q), key (K), and value (V) are obtained through linear mappings. Subsequently, applying Softmax to the query and key yields the attention scores. The final output of MSA is obtained by concatenating the outputs from all heads.

The MLP learns feature representations by projecting features into a high-dimensional space via fully connected layers and GELU operations. When the input is Y' , the computation process proceeds as follows:

$$\text{MLP}(Y') = \text{GELU} \left(Y' W^1 + b^1 \right) W^2 + b^2 \quad (6)$$

Large matrix multiplications impose a computational burden on ViT. Therefore, we choose to quantize all weights and activations of the matrix multiplication, while keeping the LayerNorm and Softmax operations at full precision.

Quantizers. The uniform quantizer (UQ) maps floating-point data to integer data and is widely used due to its hardware-friendly nature. Given the bit-width b , the processes of quantization and dequantization are as follows:

$$\text{UQ}(x, b): x_q = \text{clamp} \left(\left\lfloor \frac{x}{s} \right\rfloor + z, 0, 2^b - 1 \right) \quad (7)$$

$$\text{D-UQ}(x_q, b): x_f = s \cdot (x_q - z) \approx x \quad (8)$$

The clamp function restricts the range of the results; s denotes the scaling factor, and z represents the zero point.

$$s = \frac{\max(x) - \min(x)}{2^b - 1}, \quad z = \left\lfloor -\frac{\min(x)}{s} \right\rfloor \quad (9)$$

For post-Softmax activations, non-uniform quantizers such as the Log quantizer (LogQ) and shift-uniform-log2 quantizer (SULQ) have been proposed and widely adopted. LogQ aims to fit the distribution, while SULQ improves quantization efficiency by introducing an offset η .

$$\text{LogQ}(x, b): x_q = \text{clamp} \left(\left\lfloor -\log_2 \frac{x}{s} \right\rfloor, 0, 2^b - 1 \right) \quad (10)$$

$$\text{SULQ}(x, b): x_q = \text{UQ}(-\log_2(x + \eta), b) \quad (11)$$

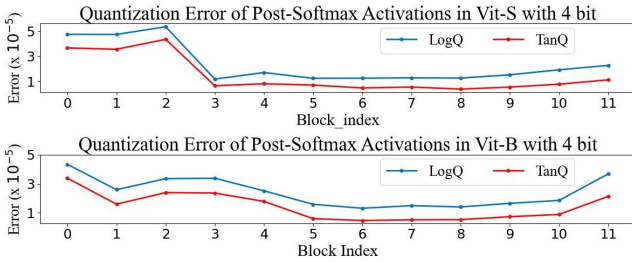


Figure 2: Comparison of Log Quantizer and Tan Quantizer for 4-bit quantization errors in post-Softmax activations.

Following earlier work, we use channel-wise quantization for weights and layer-wise quantization for activations.

Block-wise Reconstruction Optimization. Inspired by previous work (Li et al. 2021), we employ block-wise reconstruction to achieve model optimization. Here, $g(\cdot)$ represents the role of the l_{th} block, and m represents the input of the l_{th} block. By comparing the differences between the outputs of the full-precision transformer block and the quantized transformer block, we can optimize the model parameters. Block-wise reconstruction is defined as follows:

$$\mathcal{L}_l = \|g_l^f(m) - g_l^q(m)\|_2 \quad (12)$$

Reconstruction optimization is highly effective in low-bit quantization and provides a solid foundation for quantized models. However, certain components in ViTs still constrain the model’s performance. We will analyze the reasons for this limitation and propose corresponding solutions.

Distribution-Friendly Quantization for Softmax

Analysis. In ViTs, Softmax processes the query and key to obtain probability values between $[0, 1]$. These probability values are denoted as post-Softmax activations, and their distributions are neither Gaussian nor Laplace, but are characterized by long-tailed or power-law distributions. The extreme distribution of post-Softmax activations poses difficulties and challenges for quantization. Figure 1(a) shows the histogram of post-Softmax activations. It can be seen that the majority of activation values are concentrated near 0, with only a very small number of activation values approaching 1. Activation values close to 1 cannot be directly clipped as outliers; otherwise, the performance of the model will be significantly degraded. Instead, we need to pay more attention to these values because they reflect the similarity between patches. Due to the large number of activation values close to 0, it is necessary to allocate more quantization intervals to enhance differentiation. Therefore, when quantizing these activations, it is important to consider both the quantity of values near 0 and the quality of values near 1.

To keep the power-law distribution of post-Softmax activations, FQ-ViT innovatively proposes the Log2 quantizer. This quantizer allocates more quantization intervals to regions near 0, achieving superior performance compared to the uniform quantizer. However, the Log2 quantizer also suffers from quantization inefficiency due to inherent limitations. The Log2 quantizer focuses more on values near 0

but lacks emphasis on values near 1. In post-Softmax activations, values close to 1 are of high quality, while values close to 0 are of high quantity, which involves a trade-off between quality and quantity. Both uniform and Log2 quantizers allocate only a small number of quantization intervals for values close to 1, destroying the information they contain.

Tan Quantizer. Inspired by the above analysis, we propose the Tan Quantizer (TanQ) to address this issue. The quant and dequant processes of TanQ are as follows:

$$x_q = \text{clamp} \left(\left\lfloor \frac{\tan(a(x-b))}{s} \right\rfloor + z, 0, 2^b - 1 \right) \quad (13)$$

$$x_f = \arctan(\lfloor s \cdot (x_q - z) \rfloor) / a + b \approx x \quad (14)$$

The Tan Quantizer is simple and efficient, reducing emphasis on intermediate values and focusing more on values close to 0 and near 1. TanQ introduces hyperparameters a and b , which can be determined through a simple grid search method. Parameter a adjusts the curvature of the tan function, thereby influencing the number of quantization intervals allocated to values close to 0. For example, when a is larger, TanQ will allocate more quantization intervals to the region close to 0 to increase discrimination. Parameter b is responsible for adjusting the focus on values close to 1. For instance, when b is 1, we do not pay extra attention to values close to 1; when b is 0.5, we equally focus on values close to 0 and values close to 1. TanQ enhances quantization efficiency with just a slight additional computational overhead. Parameters a and b need to satisfy constraint conditions, and we formulate the optimization problem as follows:

$$\begin{aligned} & \min \|x_f - x\|_2 \\ \text{s.t. } & b + \pi/2a > 1 \\ & b - \pi/2a < 0 \\ & a > 0, b > 0, b < 1 \end{aligned} \quad (15)$$

Superiority. We present a visual comparison of the Log and the Tan Quantizer in Figure 2. The Tan Quantizer exhibits lower quantization errors and achieves superior performance. Overall, our method TanQ has two advantages.

Firstly, the Tan Quantizer effectively addresses the issue of low quantization efficiency found in other quantizers. The Tan Quantizer allocates more quantization intervals to values close to 0 and gives greater emphasis to values close to 1. This aligns well with the power-law distribution of post-Softmax activations and performs well. The Log2 and $\text{Log}\sqrt{2}$ quantizers attempt to fit the data distribution but overly focus on the precise quantization of values close to 0, neglecting those close to 1. SULQ has noticed this issue and proposed a solution, but still cannot balance the attention between values close to 0 and 1 simultaneously.

Secondly, TanQ achieves customized quantization for different post-Softmax activations. Previous uniform and Log quantizers perform the same quantization for all the post-Softmax activations in ViTs, which limits the performance. However, the Tan Quantizer adjusts its parameters to quantize different post-Softmax activations, thereby significantly improving the performance of the quantization model.

Hardware Implementation. CORDIC (Pilato, Fanucci, and Saponara 2017; Lim, Shachnai, and Nagarakatte 2020)

is an iterative algorithm that calculates the tangent value using simple addition, subtraction, and bit-shift operations. Due to its low computational complexity and hardware-friendly characteristics, it is well-suited for hardware implementation and scenarios requiring efficient computation.

Outlier-Aware Quantization for LayerNorm

Analysis. In ViTs, LayerNorm is mainly responsible for normalizing the input in the hidden feature dimension. Through analysis of post-LayerNorm activations, we find significant inter-channel variations, which pose challenges for quantization. In layer-wise quantization, a single scaling factor cannot effectively handle the inter-channel variations of post-LayerNorm activations, leading to significant degradation in accuracy. Channel-wise quantization calculates a separate scaling factor for each channel, solving this problem and ensuring the accuracy of the model. However, channel-wise quantization requires dedicated hardware support and incurs additional computational overhead. To balance the efficiency of layer-wise quantization and the accuracy of channel-wise quantization, RepQ-ViT(Li et al. 2023b) proposes the scale reparameterization method.

We have a brief overview of the whole process, and specific details can be found in RepQ-ViT. For post-LayerNorm activations with D -dimensional channels, after channel-wise quantization, we obtain scaling factors $s \in \mathbb{R}^D$ and zero points $z \in \mathbb{R}^D$. The required scaling factor and zero point for layer-wise quantization are $\tilde{s} \in \mathbb{R}^1$ and $\tilde{z} \in \mathbb{R}^1$, respectively. After defining $\tilde{s} = \tilde{s} \cdot \mathbf{1}$ and $\tilde{z} = \tilde{z} \cdot \mathbf{1}$, we can compute the variation factors $r_1 = s/\tilde{s}$ and $r_2 = z - \tilde{z}$. Therefore, we can achieve reparameterization by adjusting the affine factors of LayerNorm. Then, adjust the weights of the subsequent layer to address the activation distribution shift caused by these operations. The process is as follows:

$$\tilde{\beta} = \frac{\beta + s \odot r_2}{r_1}, \quad \tilde{\gamma} = \frac{\gamma}{r_1} \quad (16)$$

$$\tilde{W}_{:,j} = r_1 \odot W_{:,j}, \quad \tilde{b}_j = b_j - (s \odot r_2)W_{:,j} \quad (17)$$

MOSF. The scale reparameterization method balances the precision of channel-wise quantization with the efficiency of layer-wise quantization, providing a solid foundation for model quantization. However, we have found that after scale reparameterization, the model’s accuracy decreases, especially under low-bit quantization conditions. RepQ-ViT is based on rigorous mathematical derivation, so we believe the issue arises from its use of $\tilde{s} = \text{Mean}(s)$ and $\tilde{z} = \text{Mean}(z)$. As shown in Figure 1(b), some channels’ outliers can affect the average value, causing \tilde{s} to deviate from the majority of the data and lose representativeness. The key is to select the optimal scaling factor \tilde{s} required for layer-wise quantization, rather than simply calculating the average value.

We propose a method to select Median as the **Optimal Scaling Factor** named MOSF. For the D -dimensional scaling factors s , Figure 1(b) illustrates the histogram. To characterize this set of scaling factors, we can use statistics such as the maximum, minimum, mode, median, mean, and variance. Inspired by some studies(Wei et al. 2022b, 2023), we have learned that these outliers do indeed affect the model’s

performance, and overemphasizing them may actually limit the overall expressive capacity of the model. Our goal is to find a feature that can best represent the majority of the data while overcoming the influence of a small number of outliers. Mean absolute deviation (MAD) is a statistical measure of the deviation of data points from a central location. Compared to mean squared error (MSE), MAD offers greater robustness and is less sensitive to outliers. We use MAD as a metric to evaluate different statistics.

$$\text{MAD} = \frac{1}{D} \sum_{i=1}^D |s_i - \tilde{s}| \quad (18)$$

Experiments show that the \tilde{s} determined by the median results in the smallest mean absolute deviation. So MOSF proposes the best approach for finding the scaling factor required for layer-wise quantization: using the Median. The optimal \tilde{s} determined by MOSF enables precise quantization for the majority of channels, thus compensating for losses in a few abnormal channels. Although we use the scaling factor as an example, the zero point follows the same principle.

$$\tilde{s} = \text{Median}(s), \quad \tilde{z} = \text{Median}(z) \quad (19)$$

Superiority. MOSF addresses the precision degradation in the transition from channel-wise quantization to layer-wise quantization without adding any extra computational overhead. Especially in low-bit settings. MOSF can seamlessly integrate into the scale reparameterization framework of RepQ-ViT, providing comprehensive technical support for quantizing post-LayerNorm activations.

Experimentation

Experimental Setting

Models and Datasets. To validate the effectiveness of DopQ-ViT, we evaluate the image classification performance of ViT (Dosovitskiy et al. 2020), DeiT (Touvron et al. 2021), and Swin (Liu et al. 2021a) variants on the ImageNet (Russakovsky et al. 2015). Besides, we evaluate the performance of object detection and instance segmentation on the COCO (Lin et al. 2014), using Mask R-CNN (He et al. 2017) and Cascade Mask R-CNN (Cai and Vasconcelos 2018) with Swin (Liu et al. 2021a) as the backbone, respectively.

Implementation details. The pretrained full-precision models required for the experiments are obtained from the Timm library. We employ the uniform quantizer for all weights and activations, except for post-Softmax activations, which use the Tan Quantizer. We adopt the same setup as the previous method (Zhong et al. 2023a) to ensure reliable experimental results. We randomly select 1024 images from each of the ImageNet and COCO datasets for optimization. The optimization uses the Adam optimizer (Kingma and Ba 2014) with an initial learning rate and adjusts the learning rate using cosine annealing. For classification experiments on ImageNet, we set the batch size to 64 and 1000 optimization iterations for all cases, except for the 6-bit case, which is set to 200 iterations. For detection experiments on COCO, we only optimize the backbone, set the batch size to 1, and adopt 1000 optimization iterations. The parameters in the Tan Quantizer are obtained using a simple grid search.

Method	Opti.	Bit. (W/A)	ViT-S	ViT-B	DeiT-T	DeiT-S	DeiT-B	Swin-S	Swin-B
Full-Precision	-	32/32	81.39	84.54	72.21	79.85	81.80	83.23	85.27
BRECQ (Li et al. 2021)	✓	3/3	0.42	0.59	25.52	14.63	46.29	11.67	1.70
QDrop (Wei et al. 2022a)	✓	3/3	4.44	8.00	30.73	22.67	24.37	60.89	54.76
PD-Quant (Liu et al. 2023)	✓	3/3	1.77	13.09	39.97	29.33	0.94	69.67	64.32
RepQ-ViT (Li et al. 2023b)	×	3/3	0.43	0.14	0.97	4.37	4.84	8.84	1.34
I&S-ViT (Zhong et al. 2023a)	✓	3/3	45.16	63.77	41.52	55.78	73.30	74.20	69.30
DopQ-ViT (ours)	✓	3/3	54.72	65.76	44.71	59.26	74.91	74.77	69.63
BRECQ (Li et al. 2021)	✓	4/4	12.36	9.68	55.63	63.73	72.31	72.74	58.24
QDrop (Wei et al. 2022a)	✓	4/4	21.24	47.30	61.93	68.27	72.60	79.58	80.93
PD-Quant (Liu et al. 2023)	✓	4/4	1.51	32.45	62.46	71.21	73.76	79.87	81.12
RepQ-ViT (Li et al. 2023b)	×	4/4	65.05	68.48	57.43	69.03	75.61	79.45	78.32
I&S-ViT (Zhong et al. 2023a)	✓	4/4	74.87	80.07	65.21	75.81	79.97	81.17	82.60
DopQ-ViT (ours)	✓	4/4	75.69	80.95	65.54	75.84	80.13	81.71	83.34
BRECQ (Li et al. 2021)	✓	6/6	54.51	68.33	70.28	78.46	80.85	82.02	83.94
QDrop (Wei et al. 2022a)	✓	6/6	70.25	75.76	70.64	77.95	80.87	82.60	84.33
PD-Quant (Liu et al. 2023)	✓	6/6	70.84	75.82	70.49	78.40	80.52	82.51	84.32
RepQ-ViT (Li et al. 2023b)	×	6/6	80.43	83.62	70.76	78.90	81.27	82.79	84.57
I&S-ViT (Zhong et al. 2023a)	✓	6/6	80.43	83.82	70.85	79.15	81.68	82.89	84.94
DopQ-ViT (ours)	✓	6/6	80.52	84.02	71.17	79.30	81.69	82.95	84.97

Table 1: Quantization results for image classification on the ImageNet dataset. ‘‘Opti.’’ represents the optimization-based approach. ‘‘Bit. (W/A)’’ denotes the quantization bit-width of weights and activations as W bits and A bits, respectively.

Method	Opti.	Bit. (W/A)	Mask R-CNN				Cascade Mask R-CNN			
			w. Swin-T		w. Swin-S		w. Swin-T		w. Swin-S	
			AP ^{box}	AP ^{mask}	AP ^{box}	AP ^{mask}	AP ^{box}	AP ^{mask}	AP ^{box}	AP ^{mask}
Full-Precision	-	32/32	46.0	41.6	48.5	43.3	50.4	43.7	51.9	45.0
BRECQ (Li et al. 2021)	✓	4/4	25.4	27.6	34.9	35.4	41.2	37.0	44.5	39.2
QDrop (Wei et al. 2022a)	✓	4/4	12.4	12.9	42.7	40.2	23.9	21.2	24.1	21.4
PD-Quant (Liu et al. 2023)	✓	4/4	17.7	18.1	32.2	30.9	35.5	31.0	41.6	36.3
RepQ-ViT (Li et al. 2023b)	×	4/4	36.1	36.0	42.7*	40.1*	47.0	41.4	49.3	43.1
I&S-ViT (Zhong et al. 2023a)	✓	4/4	37.5	36.6	43.4	40.3	48.2	42.0	50.3	43.6
DopQ-ViT (Ours)	✓	4/4	37.5	36.5	43.5	40.4	48.2	42.1	50.3	43.7

Table 2: Quantization results on the COCO . ‘‘AP^{box}’’ represents the box average precision for object detection, and ‘‘AP^{mask}’’ represents the mask average precision for instance segmentation. ‘‘*’’ denotes that the result are obtained from the official code.

Results on ImageNet Dataset

We evaluated the performance of DopQ-ViT on the ImageNet dataset for image classification and compared it with other methods, as shown in Table 1. In comparison with other methods, DopQ-ViT achieves outstanding performance across different ViT variants and bit settings. In the 3-bit case, nearly all methods fail; for instance, RepQ-ViT fails across all ViT variants. Optimization-based methods, such as BRECQ, QDrop, and PD-Quant, put in more effort but only enhance the performance of certain ViT variants. I&S-ViT is the first to improve the 3-bit quantization performance of various ViT variants to a practical level. However, it still falls short of the full-precision model, which has motivated the DopQ-ViT on low-bit quantization. DopQ-ViT not only improves the accuracy of the 3-bit quantization but also demonstrates stability across various variants. Specifically, on ViT-S and ViT-B, DopQ-ViT achieves Top-1 accuracy of 54.72% and 65.76%, respectively, with an

improvement of 9.56% and 1.99% compared to I&S-ViT. For DeiT-T, DeiT-S, and DeiT-B, DopQ-ViT achieves Top-1 accuracy of 44.71%, 59.26%, and 74.91%, respectively, with improvements of 3.19%, 3.48%, and 1.61% compared to I&S-ViT. On Swin-S and Swin-B, DopQ-ViT achieves Top-1 accuracy of 74.77% and 69.63%, respectively. In the 4-bit case, RepQ-ViT achieves more effective quantization for Softmax and LayerNorm, resulting in superior performance. I&S-ViT further improves quantization efficiency and narrows the gap with full-precision models using reconstruction. It is worth noting that DopQ-ViT further enhances the performance and practicality of 4-bit quantized models. Specifically, it achieves Top-1 accuracy of 75.69% and 80.95% for ViT-S and ViT-B, and 65.54%, 75.84%, and 80.13% for DeiT-T, DeiT-S, and DeiT-B, respectively. In the 6-bit case, DopQ-ViT achieves nearly lossless performance in quantization. Compared to the full-precision models, the Top-1 accuracy of DeiT-B decreases by only 0.11%.

Model	Bit.(W/A)	Method			
		Uniform	LogQ	SULQ	TanQ
DeiT-B	W32/A32	81.80	81.80	81.80	81.80
	W32/A3	0.25	34.11	68.04	70.93

Table 3: Ablation studies of different quantizers for post-Softmax activations in 3-bit quantization of DeiT-B.

Quantization	Method	Model			
		ViT-S	ViT-B	DeiT-T	DeiT-S
Channel-wise	W32/A3	55.70	68.51	46.49	67.66
↓Reparam	w. RepQ	40.88	61.66	42.76	64.06
Layer-wise	w. MOSF	55.71	68.52	46.65	67.79

Table 4: Ablation studies of prior scaling factor determination (RepQ) and Median as Optimal Scaling Factor (MOSF) in 3-bit quantization for post-LayerNorm activations.

Model	Bit.(W/A)	Method (TanQ, MOSF)			
		(\times , \times)	(\times , \checkmark)	(\checkmark , \times)	(\checkmark , \checkmark)
ViT-S	W3/A3	53.56	54.67	53.63	54.72
DeiT-B	W3/A3	74.28	74.39	74.77	74.91

Table 5: Ablation studies on the effectiveness of the Tan Quantizer (TanQ) and Median as the Optimal Scaling Factor (MOSF) based on the current state-of-the-art method.

Results on COCO Dataset

Object detection and instance segmentation experiments were conducted on the COCO dataset, with the results shown in Table 2. The model architecture for these tasks is more complex, which makes quantization challenging, but DopQ-ViT still achieves good performance. We conduct experiments in the W4A4 quantization setting. Specifically, with Swin-T as the backbone of Mask R-CNN, the box AP and mask AP are 37.5% and 36.5%, respectively. With Swin-S as the backbone, the box AP and mask AP are 43.5% and 40.4%, respectively. Similarly, with Swin-T as the backbone of Cascade Mask R-CNN, the box AP and mask AP are 48.2% and 42.1%, respectively. With Swin-S as the backbone, the box AP and mask AP are 50.3% and 43.7%, respectively. Even compared to other existing methods, DopQ-ViT still performs impressively.

Ablation Studies

Effect of TanQ for post-Softmax activations We use the uniform quantizer to quantize the activations of the full-precision DeiT-B model to 3 bit, with only the post-Softmax activations using the separate quantizer. Detailed experimental results are shown in Table 3. It’s evident that the uniform quantizer is completely ineffective in 3-bit quantization. LogQ can adapt to the distribution of post-Softmax activations, thereby improving the model’s performance. SULQ further enhances quantization efficiency, making low-bit

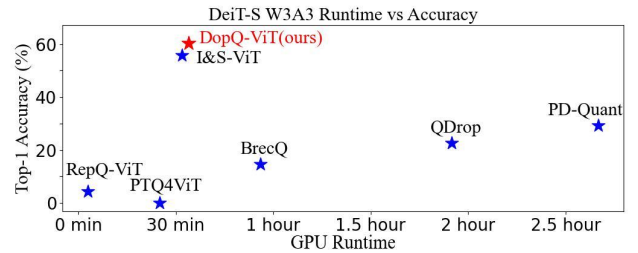


Figure 3: The runtime vs. accuracy of PTQ methods.

quantization more practical. Our method TanQ achieves the Top-1 accuracy of 70.93%, which further improves the performance of the low-level quantization model.

Effect of MOSF for post-LayerNorm activations We validate the effectiveness of MOSF through 3-bit quantization experiments across various models, with detailed results shown in Table 4. “RepQ” represents the traditional method for determining a single scaling factor for layer-wise quantization. Compared to RepQ, MOSF effectively mitigates accuracy degradation caused by reparameterization. With the help of MOSF, each model achieves nearly lossless results after reparameterizing from channel-wise quantization to layer-wise quantization.

Effect of TanQ and MOSF We conduct ablation studies on the proposed TanQ and MOSF, and the results are shown in Table 5. Using the current SOTA method as a baseline, TanQ and MOSF still show advantages. Combining TanQ and MOSF, ViT-S and DeiT-B achieve 54.72% and 74.91% Top-1 accuracy, respectively, showing the best performance.

Time efficiency Figure 3 illustrates the runtime and accuracy of post-training quantization methods. DopQ-ViT performs better in time efficiency compared to optimization-based PTQ methods and demonstrates superior accuracy compared to other direct post-training quantization methods.

Conclusion

In this paper, we analyze the reasons behind the poor performance of existing post-training quantization methods for vision transformers. To address these issues, we propose a distribution-friendly and outlier-aware PTQ method named DopQ-ViT. We find that current quantization paradigms do not align well with the power-law distribution of post-Softmax activations. Therefore, we propose the Tan Quantizer to better focus on values close to 1. We also perceive that model performance decreases during the transition from channel-wise to layer-wise quantization of post-LayerNorm activations. This is influenced by outliers in the scaling factors. Therefore, we propose MOSF to select Median as the optimal scaling factor, which mitigates the impact of a few abnormal channels by accurately quantizing the majority of channels. We evaluate DopQ-ViT across different ViT variants and bit settings in classification and detection tasks. The experimental results indicate that DopQ-ViT has a competitive advantage over other post-training quantization methods and further enhances the practicality of quantized models.

References

- Banner, R.; Nahshan, Y.; and Soudry, D. 2019. Post training 4-bit quantization of convolutional networks for rapid-deployment. *Advances in Neural Information Processing Systems*, 32.
- Bhojanapalli, S.; Chakrabarti, A.; Glasner, D.; Li, D.; Unterthiner, T.; and Veit, A. 2021. Understanding robustness of transformers for image classification. In *Proceedings of the IEEE/CVF international conference on computer vision*, 10231–10241.
- Cai, Z.; and Vasconcelos, N. 2018. Cascade r-cnn: Delving into high quality object detection. In *Proceedings of the IEEE/CVF Conference on Computer Vision and Pattern Recognition (CVPR)*, 6154–6162.
- Carion, N.; Massa, F.; Synnaeve, G.; Usunier, N.; Kirillov, A.; and Zagoruyko, S. 2020. End-to-end object detection with transformers. In *European conference on computer vision*, 213–229. Springer.
- Chen, C.-F. R.; Fan, Q.; and Panda, R. 2021. Crossvit: Cross-attention multi-scale vision transformer for image classification. In *Proceedings of the IEEE/CVF international conference on computer vision*, 357–366.
- Chen, W.; Du, X.; Yang, F.; Beyer, L.; Zhai, X.; Lin, T.-Y.; Chen, H.; Li, J.; Song, X.; Wang, Z.; et al. 2021. A simple single-scale vision transformer for object localization and instance segmentation. *arXiv preprint arXiv:2112.09747*.
- Choi, J.; Wang, Z.; Venkataramani, S.; Chuang, P. I.-J.; Srinivasan, V.; and Gopalakrishnan, K. 2018. Pact: Parameterized clipping activation for quantized neural networks. *arXiv preprint arXiv:1805.06085*.
- Ding, Y.; Qin, H.; Yan, Q.; Chai, Z.; Liu, J.; Wei, X.; and Liu, X. 2022. Towards Accurate Post-Training Quantization for Vision Transformer. In *Proceedings of the 30th ACM International Conference on Multimedia*, 5380–5388.
- Dosovitskiy, A.; Beyer, L.; Kolesnikov, A.; Weissenborn, D.; Zhai, X.; Unterthiner, T.; Dehghani, M.; Minderer, M.; Heigold, G.; Gelly, S.; et al. 2020. An image is worth 16x16 words: Transformers for image recognition at scale. *arXiv preprint arXiv:2010.11929*.
- Esser, S. K.; McKinstry, J. L.; Bablani, D.; Appuswamy, R.; and Modha, D. S. 2019. Learned step size quantization. *arXiv preprint arXiv:1902.08153*.
- Frumkin, N.; Gope, D.; and Marculescu, D. 2023. Jumping through local minima: Quantization in the loss landscape of vision transformers. In *Proceedings of the IEEE/CVF International Conference on Computer Vision*, 16978–16988.
- Gholami, A.; Kim, S.; Dong, Z.; Yao, Z.; Mahoney, M. W.; and Keutzer, K. 2022. A survey of quantization methods for efficient neural network inference. In *Low-Power Computer Vision*, 291–326. Chapman and Hall/CRC.
- Gong, R.; Liu, X.; Jiang, S.; Li, T.; Hu, P.; Lin, J.; Yu, F.; and Yan, J. 2019. Differentiable soft quantization: Bridging full-precision and low-bit neural networks. In *Proceedings of the IEEE/CVF international conference on computer vision*, 4852–4861.
- He, K.; Gkioxari, G.; Dollár, P.; and Girshick, R. 2017. Mask r-cnn. In *Proceedings of the IEEE/CVF International Conference on Computer Vision (ICCV)*, 2961–2969.
- Kingma, D. P.; and Ba, J. 2014. Adam: A method for stochastic optimization. *arXiv preprint arXiv:1412.6980*.
- Krishnamoorthi, R. 2018. Quantizing deep convolutional networks for efficient inference: A whitepaper. *arXiv preprint arXiv:1806.08342*.
- Li, Y.; Gong, R.; Tan, X.; Yang, Y.; Hu, P.; Zhang, Q.; Yu, F.; Wang, W.; and Gu, S. 2021. BRECQ: Pushing the Limit of Post-Training Quantization by Block Reconstruction. In *Proceedings of the International Conference on Learning Representations (ICLR)*.
- Li, Y.; Mao, H.; Girshick, R.; and He, K. 2022a. Exploring plain vision transformer backbones for object detection. In *European conference on computer vision*, 280–296. Springer.
- Li, Y.; Xu, S.; Zhang, B.; Cao, X.; Gao, P.; and Guo, G. 2022b. Q-vit: Accurate and fully quantized low-bit vision transformer. *Advances in neural information processing systems*, 35: 34451–34463.
- Li, Z.; Chen, M.; Xiao, J.; and Gu, Q. 2023a. PSAQ-ViT v2: Toward accurate and general data-free quantization for vision transformers. *IEEE Transactions on Neural Networks and Learning Systems*.
- Li, Z.; and Gu, Q. 2023. I-vit: Integer-only quantization for efficient vision transformer inference. In *Proceedings of the IEEE/CVF International Conference on Computer Vision*, 17065–17075.
- Li, Z.; Ma, L.; Chen, M.; Xiao, J.; and Gu, Q. 2022c. Patch similarity aware data-free quantization for vision transformers. In *European conference on computer vision*, 154–170. Springer.
- Li, Z.; Xiao, J.; Yang, L.; and Gu, Q. 2023b. Repq-vit: Scale reparameterization for post-training quantization of vision transformers. In *Proceedings of the IEEE/CVF International Conference on Computer Vision*, 17227–17236.
- Li, Z.; Yang, T.; Wang, P.; and Cheng, J. 2022d. Q-vit: Fully differentiable quantization for vision transformer. *arXiv preprint arXiv:2201.07703*.
- Lim, J. P.; Shachnai, M.; and Nagarakatte, S. 2020. Approximating trigonometric functions for posits using the CORDIC method. In *Proceedings of the 17th ACM International Conference on Computing Frontiers*, 19–28.
- Lin, T.-Y.; Maire, M.; Belongie, S.; Hays, J.; Perona, P.; Ramanan, D.; Dollár, P.; and Zitnick, C. L. 2014. Microsoft coco: Common objects in context. In *Computer Vision—ECCV 2014: 13th European Conference, Zurich, Switzerland, September 6–12, 2014, Proceedings, Part V 13*, 740–755. Springer.
- Lin, Y.; Zhang, T.; Sun, P.; Li, Z.; and Zhou, S. 2022. FQ-ViT: Post-Training Quantization for Fully Quantized Vision Transformer. In Raedt, L. D., ed., *Proceedings of the Thirty-First International Joint Conference on Artificial Intelligence, (IJCAI)*, 1173–1179.

- Liu, C.; Shi, H.; and He, X. 2023. FGPTQ-ViT: Fine-Grained Post-training Quantization for Vision Transformers. In *Chinese Conference on Pattern Recognition and Computer Vision (PRCV)*, 79–90. Springer.
- Liu, J.; Niu, L.; Yuan, Z.; Yang, D.; Wang, X.; and Liu, W. 2023. Pd-quant: Post-training quantization based on prediction difference metric. In *Proceedings of the IEEE/CVF Conference on Computer Vision and Pattern Recognition*, 24427–24437.
- Liu, S.-Y.; Liu, Z.; and Cheng, K.-T. 2023. Oscillation-free quantization for low-bit vision transformers. In *International Conference on Machine Learning*, 21813–21824. PMLR.
- Liu, Z.; Lin, Y.; Cao, Y.; Hu, H.; Wei, Y.; Zhang, Z.; Lin, S.; and Guo, B. 2021a. Swin transformer: Hierarchical vision transformer using shifted windows. In *Proceedings of the IEEE/CVF international conference on computer vision (ICCV)*, 10012–10022.
- Liu, Z.; Ning, J.; Cao, Y.; Wei, Y.; Zhang, Z.; Lin, S.; and Hu, H. 2022. Video swin transformer. In *Proceedings of the IEEE/CVF conference on computer vision and pattern recognition*, 3202–3211.
- Liu, Z.; Wang, Y.; Han, K.; Zhang, W.; Ma, S.; and Gao, W. 2021b. Post-training quantization for vision transformer. *Advances in Neural Information Processing Systems*, 34: 28092–28103.
- Nagel, M.; Fourarakis, M.; Bondarenko, Y.; and Blankevoort, T. 2022. Overcoming oscillations in quantization-aware training. In *International Conference on Machine Learning*, 16318–16330. PMLR.
- Pilato, L.; Fanucci, L.; and Saponara, S. 2017. Real-time and high-accuracy arctangent computation using CORDIC and fast magnitude estimation. *Electronics*, 6(1): 22.
- Russakovsky, O.; Deng, J.; Su, H.; Krause, J.; Satheesh, S.; Ma, S.; Huang, Z.; Karpathy, A.; Khosla, A.; Bernstein, M.; et al. 2015. ImageNet Large Scale Visual Recognition Challenge. *International Journal of Computer Vision (IJCV)*, 115: 211–252.
- Touvron, H.; Cord, M.; Douze, M.; Massa, F.; Sablayrolles, A.; and Jégou, H. 2021. Training data-efficient image transformers & distillation through attention. In *International conference on machine learning*, 10347–10357. PMLR.
- Wang, Y.; Xu, Z.; Wang, X.; Shen, C.; Cheng, B.; Shen, H.; and Xia, H. 2021. End-to-end video instance segmentation with transformers. In *Proceedings of the IEEE/CVF conference on computer vision and pattern recognition*, 8741–8750.
- Wei, X.; Gong, R.; Li, Y.; Liu, X.; and Yu, F. 2022a. QDrop: Randomly Dropping Quantization for Extremely Low-bit Post-Training Quantization. In *Proceedings of the International Conference on Learning Representations (ICLR)*.
- Wei, X.; Zhang, Y.; Li, Y.; Zhang, X.; Gong, R.; Guo, J.; and Liu, X. 2023. Outlier suppression+: Accurate quantization of large language models by equivalent and optimal shifting and scaling. *arXiv preprint arXiv:2304.09145*.
- Wei, X.; Zhang, Y.; Zhang, X.; Gong, R.; Zhang, S.; Zhang, Q.; Yu, F.; and Liu, X. 2022b. Outlier suppression: Pushing the limit of low-bit transformer language models. *Advances in Neural Information Processing Systems*, 35: 17402–17414.
- Wu, K.; Zhang, J.; Peng, H.; Liu, M.; Xiao, B.; Fu, J.; and Yuan, L. 2022. Tinyvit: Fast pretraining distillation for small vision transformers. In *European conference on computer vision*, 68–85. Springer.
- Yang, L.; Li, Z.; Xiao, J.; Gong, H.; and Gu, Q. 2024. MGRQ: Post-Training Quantization For Vision Transformer With Mixed Granularity Reconstruction. *arXiv preprint arXiv:2406.09229*.
- Yu, F.; Huang, K.; Wang, M.; Cheng, Y.; Chu, W.; and Cui, L. 2022. Width & depth pruning for vision transformers. In *Proceedings of the AAAI Conference on Artificial Intelligence*, volume 36, 3143–3151.
- Yuan, L.; Chen, Y.; Wang, T.; Yu, W.; Shi, Y.; Jiang, Z.-H.; Tay, F. E.; Feng, J.; and Yan, S. 2021. Tokens-to-token vit: Training vision transformers from scratch on imagenet. In *Proceedings of the IEEE/CVF international conference on computer vision*, 558–567.
- Yuan, Z.; Xue, C.; Chen, Y.; Wu, Q.; and Sun, G. 2022. Ptq4vit: Post-training quantization for vision transformers with twin uniform quantization. In *European Conference on Computer Vision*, 191–207. Springer.
- Zhong, Y.; Hu, J.; Lin, M.; Chen, M.; and Ji, R. 2023a. I&S-ViT: An Inclusive & Stable Method for Pushing the Limit of Post-Training ViTs Quantization. *arXiv preprint arXiv:2311.10126*.
- Zhong, Y.; Lin, M.; Li, X.; Li, K.; Shen, Y.; Chao, F.; Wu, Y.; and Ji, R. 2022. Dynamic dual trainable bounds for ultra-low precision super-resolution networks. In *European Conference on Computer Vision*, 1–18. Springer.
- Zhong, Y.; Lin, M.; Zhou, Y.; Chen, M.; Zhang, Y.; Chao, F.; and Ji, R. 2023b. MultiQuant: A Novel Multi-Branch Topology Method for Arbitrary Bit-width Network Quantization. *arXiv preprint arXiv:2305.08117*.